HOKKAIDO UNIVERSITY

Title	Room-temperature electric field control of spin filtering efficiency for enhanced modulation of optical spin polarization in a defect-functional 0D-2D hybrid nanostructure
Author(s)	Park, Soyoung; Hiura, Satoshi; Kise, Hiroto et al.
Citation	Nanoscale, 15(41), 16784-16794 https://doi.org/10.1039/d3nr03438k
Issue Date	2023-11-07
Doc URL	https://hdl.handle.net/2115/93132
Type	journal article
File Information	Revised manuscript_clean.pdf

Hokkaido University Collection of Scholarly and Academic Papers : HUSCAP

Room-temperature electric field control of spin filtering efficiency for enhanced modulation of optical spin polarization in a defect-functional 0D-2D hybrid nanostructure

Soyoung Park, Satoshi Hiura*, Hiroto Kise, Junichi Takayama, Kazuhisa Sueoka, and Akihiro Murayama

Faculty of Information Science and Technology, Hokkaido University, 060-0814, Japan
*Correspondence: hiura@ist.hokudai.ac.jp

Keywords: quantum dots; spin filter; spin polarization; electric field effect; photoluminescence

Abstract

In order to accomplish spin-based photoelectric information processing, it is necessary to modulate electron spin polarization in III-V semiconductor quantum dots (QDs) using an electric field. However, there is a principal limitation to the spin polarization degree and its control range, as the electron spin polarization is rapidly lost during injection into the QDs at room temperature (RT). Here, electric field control of optical spin polarization in the range of 15–40% is demonstrated at RT using InAs QDs tunnel-coupled with a defect-functional GaNAs quantum well (QW) spin filter. This compares with an electric field control of 1–4% for InAs QDs tunnel-coupled with an InGaAs QW. Transient polarization in the range of 30–60% is also obtained in the ultrafast time domain of less than 100 ps, the degree of polarization depending on the electric field. The enhanced polarization control is achieved by tuning the amplified spin polarization of electrons tunnel-injected from the GaNAs QW into QDs via the electric-field-dependent spin-filtering efficiency of GaNAs. These findings will provide a new way to extensively modulate the electron spin polarization in opto-semiconductors, by electric-field-induced on/off switching of spin amplification.

Introduction

For the development of advanced information systems, semiconductor spintronics has been expected to improve the performance of classical electronic devices by utilizing the spin degree of freedom of electrons, overcoming the limitation of Moore's law.[1-4] The generation and manipulation of electron spins in semiconductors play a key role in not only exploring the fundamental spin properties but also in achieving breakthroughs in the emerging semiconductor spintronics. This electron spin information can result in fast data processing and a long storage time with ultralow power consumption.[5] In semiconductors, spin-polarized electrons recombine radiatively with holes and emit circularly polarized light. In this process, the circular polarization property of light reflects the electron spin polarization via photoelectric conversion, according to the optical-transition selection rule.[6] An optical spin device that seamlessly converts information between electron spin information and optical spin information is a key technology for future spin-based photoelectric information processing systems. This spin-based information system can be used to achieve ultra-low-power operation, fast data transmission, and low transmission loss.

On the other hand, electron spin information is easily lost during spin transport in semiconductors owing to several spin relaxation mechanisms, such as the Dyakonov-Perel (DP),[7,8] Elliot-Yaffet,[9,10] and Bir-Aronov-Pikus mechanisms.[11] III-V semiconductor QDs are promising nanomaterials for the active layer of optical spin devices because of their significant suppression of spin relaxation,[12-14] and superior optical properties,[15-17] owing to their three-dimensional quantum confinement. Manipulation of optical spin polarization in semiconductor nanomaterials has been achieved with the application of a magnetic field via Zeeman splitting.[18-21] However, a strong magnetic field of 35 T was required to control the electron spin polarization at room temperature (RT) because of the large thermal distribution between the Zeeman split levels.[22] It is desirable to perform electric field control of electron spin polarization without requiring a magnetic field for practical device applications in

semiconductor spintronics.[23,24] The circular polarization degree of photoluminescence (PL), corresponding to the spin polarization degree of electrons, has been controlled by an electric field using InGaAs QW–QD tunnel-coupled structures.[25,26] Efficient RT voltage control of PL circular polarization in the range of 3–15 % has recently been demonstrated.[27] However, for such an InGaAs-based nanostructure, the PL intensity decreases significantly at RT because of the dominant thermal escape of electrons from the QDs to the barrier.[28] Furthermore, the electron spin polarization of the QDs decreases because of the reinjection of electron spins that are rapidly depolarized in the surrounding GaAs barriers.[29,30] Therefore, the enhancement of QD electron spin polarization and QD luminescence intensity at RT is required for practical applications of electric field-effect optical spin devices using QDs.

In this study, we focus on a hybrid nanosystem comprising a dilute nitride GaNAs QW tunnel-coupled to InAs QDs via a thin GaAs tunneling barrier. In general, InAs/GaAs QDs have a larger band offset than InGaAs/GaAs QDs, which can suppress the thermal escape of carriers. More importantly, the electron spin polarization of QDs was recently found to significantly increase with temperature, up to RT, using the GaNAs QW-InAs QD tunnel-coupled structure.[31] The amplification of spin polarization originated from thermally-accelerated remote spin filtering via deep-level defects in GaNAs. The highest RT electron spin polarization ever reported for semiconductors of up to 90 % was achieved. In GaNAs, Ga self-interstitials act as spin-polarized spin-filtering defects because of thermally activated spin-dependent recombination (SDR).[32,33] Spin-polarized defects selectively capture conduction-band electrons with a spin orientation opposite to that of the defect electrons, enhancing the spin polarization of conduction-band electrons. In this study, we fabricated an electric-field-effect optical spin device using a tunnel-coupled nanostructure of defect-functional GaNAs QW and InAs QDs, in which the electron wavefunction can be strongly coupled between GaNAs and the QD excited state (ES). Electric field control of QD PL polarization in the range of 15–40% is

demonstrated at RT. We also demonstrate that the PL polarization change is attributed to the electric-field-dependent spin-filtering efficiency of the GaNAs QW.

Results and discussion

Fig. 1(a) shows a schematic of the electric-field-effect optical spin device used in this study. A single layer of 3.8-ML-thick InAs QDs was grown on a 5-nm-thick-GaNAs QW via a 3-nm-thick GaAs tunneling barrier. The $Al_{0.2}Ga_{0.8}As$ barriers behave as carrier-blocking layers and

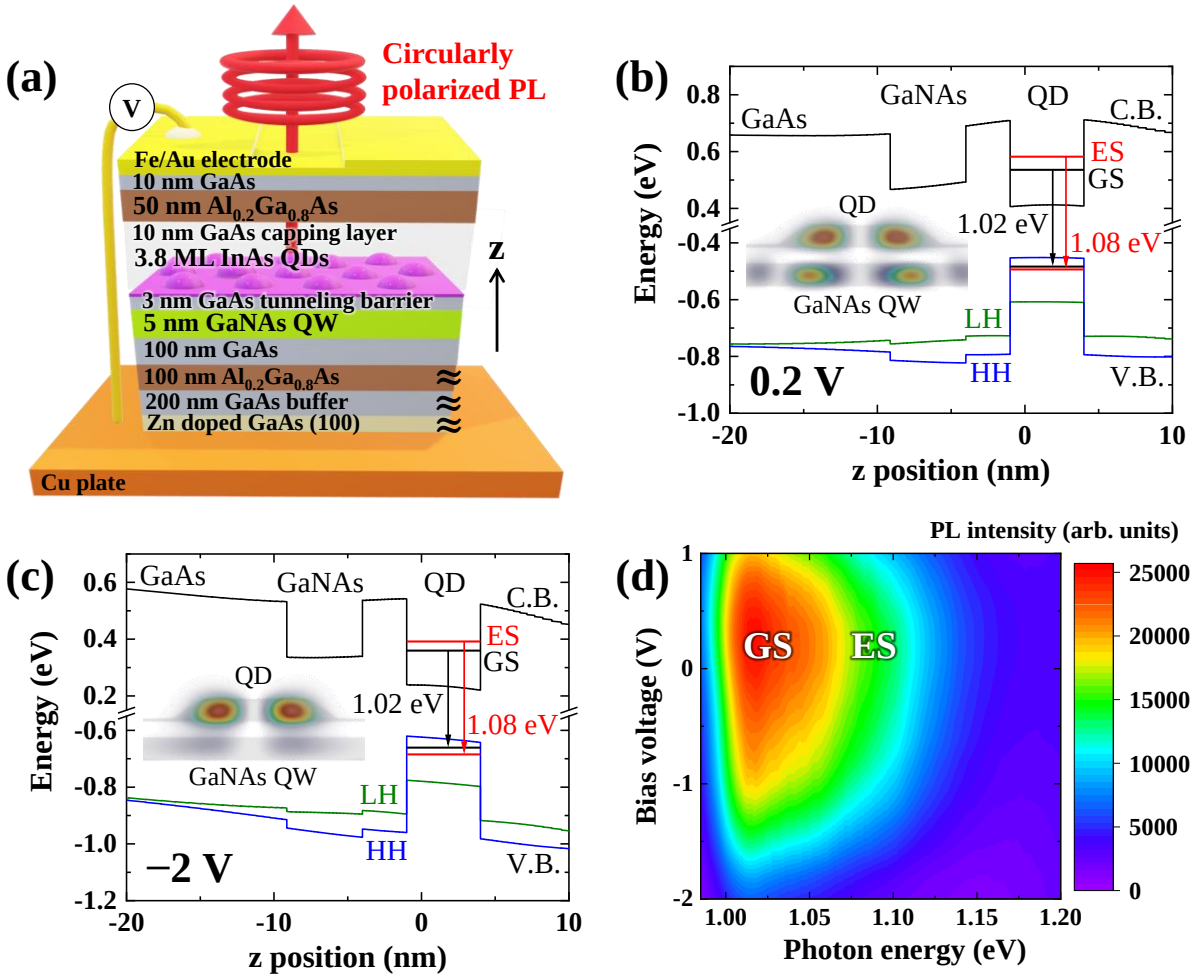


Fig. 1 Electric-field-effect optical spin device using InAs QDs tunnel-coupled with a 5-nm-thick GaNAs QW. (a) Schematic illustration of device and sample structure. Three-dimensional calculated band profiles of the GaNAs QW-InAs QD tunnel-coupled structure with bias voltages of (b) 0.2 V and (c) −2 V. The inset of each figure shows the typical spatial maps of the existence probabilities of electron wavefunctions (*p* orbitals) at the QD ES. (d) A contour map indicating bias voltage dependence of QD PL intensity as a function of photon energy at 295 K.

can confine carriers in the active layer.[26] An external bias voltage was applied along the growth direction for the electric field control of the band potential. The electric field effects on the three-dimensional band potential of the GaNAs QW-InAs QD tunnel-coupled structure were calculated using nextnano software.[34] The details of the calculation model are described in the Experimental Section. Figs. 1(b) and 1(c) show the one-dimensional potential along the growth direction at the center position of a QD at bias voltages of 0.2 V and −2 V, respectively. The energy positions of the QD states and typical spatial maps of the electron wavefunctions at the QD ES are also shown. A nearly flat band potential was reached at a bias voltage of 0.2 V. The flat band potential at around 0.2 V was also experimentally demonstrated by investigating the bias voltage dependence of the photocurrent (see supplementary Note S1, Supporting Information). In this study, spin-polarized carriers were predominantly generated in a 100-nm-thick GaAs layer grown below the GaNAs QW. The optically-generated electrons are directly injected into the QDs or captured by the GaNAs QW, and subsequently injected into the QDs. However, the generated holes are likely to be directly injected into the QDs. Under this flat band condition, both electrons and holes are efficiently injected into the QDs, resulting in a high QD PL intensity [Fig. 1(d)]. It can be clearly seen in Fig. 1(b) that the electron wavefunction of the QD ES spreads significantly over the GaNAs QW. This simulation result indicates that electrons can move back and forth between the GaNAs QW and QD ES via spin-conserving tunneling.

On the other hand, at a bias voltage of −2 V, the conduction band potential has a distinct tilt toward the QD side of the structure, whereas the valence band potential exhibits the opposite behavior. Under these conditions, holes are less likely to be injected into the QDs because of the tilted potential; however, electrons injected into the QDs are more likely to tunnel escape to the GaAs capping layer via thermal excitation. As a result, both electrons and holes inside the QDs are absent, leading to a decrease in the QD PL intensity [Fig. 1(d)]. Note that the spread of the QD ES electron wavefunction over the GaNAs QW became much weaker [Fig. 1(c)]. In

this case, the contribution of the GaNAs spin filter to the QD PL properties should be small. These simulation results suggest that the coupling strength of the electron wavefunctions between the GaNAs QW and QD ES can be controlled by changing the bias voltage.

Next, the electric field effects on the QD PL polarization are investigated. Figs. 2(a) and 2(b) show the circularly polarized PL spectra and the corresponding PL polarizations at bias voltages of −2 V and 0.2 V, respectively. Here, $\sigma^{\pm}$ indicates the co- and cross-circularly polarized PL intensities with σ^{+}-polarized excitation. The peak-fitting analysis of the PL spectrum at 0.2 V reveals four peaks of around 1.01, 1.04, 1.08, and 1.13 eV (Fig. S2). The former two peaks indicate the presence of the QD ground state (GS), including the size nonuniformity of the QD ensembles (Fig. S3). The peak of 1.08 eV indicates the presence of

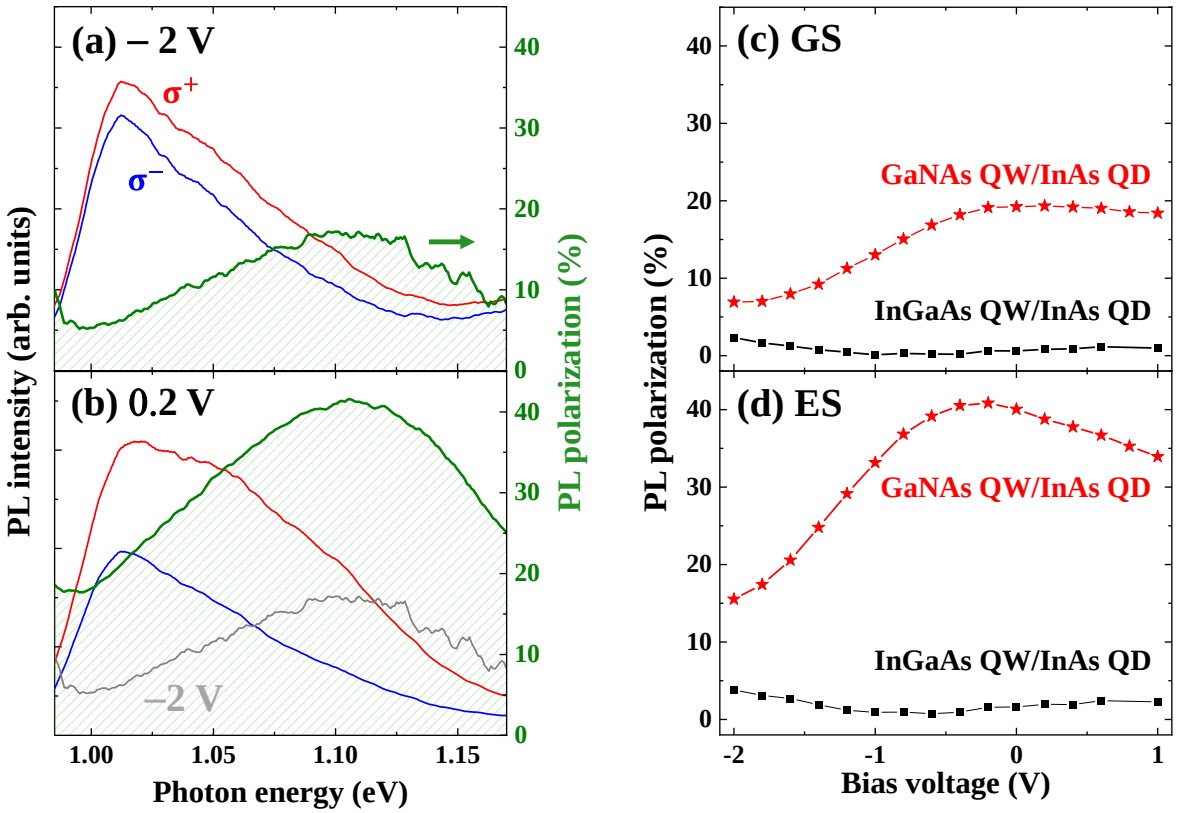


Fig. 2 Bias voltage dependence of QD PL polarization. Circularly-polarized PL spectra and corresponding PL polarization of QDs measured at 295 K with bias voltages of (a) −2 V and (b) 0.2 V. The gray line shown in (b) indicates the PL polarization with a bias voltage of −2 V to compare with the 0.2 V bias voltage results. Bias voltage dependence of PL polarization at (c) the QD GS and (d) the QD ES for the GaNAs QW-InAs QD tunnel-coupled structure, in comparison with those for InGaAs QW-InAs QD tunnel-coupled structure.

the first excited states of these QD ensembles. The higher-energy peak of 1.13 eV may indicate the second excited states and higher-energy excited states. The broad PL spectrum ranging from 0.95 to 1.15 eV is attributed to the relatively strong excitation power used, which means that carriers can be distributed to the high-energy excited states. A contour map of the QD PL intensity as a function of photon energy and bias voltage is shown in Fig. 1(d). PL emission from the QD GS and the QD ES was measured to have photon energies of 1.02 eV and 1.08 eV, respectively [Fig. 1(b)]. The relatively strong PL from the QD ES around 0 V reflects a strong coupling between the GaNAs and the QD ES. Based on a previous study,[31] the observed QD PL spectra tend to have a large contribution from QD states that are strongly coupled with GaNAs states. The gradual decrease in the PL intensity from 0.2 V to 1 V can be attributed to the suppression of electrons being injected into the QDs by the tilting of the conduction band potential toward the GaNAs QW.

As described above, a clear difference in the PL intensity appears when changing the bias voltage between 0.2 V and −2 V. The bias-voltage dependence of the QD PL intensity has been previously discussed based on the electric-field-dependent absence of electrons or holes inside the QDs.[25-27] It should be noted that there was also a significant difference in the PL polarization over a wide energy range. Figs. 2(c) and 2(d) show the PL polarization as a function of the bias voltage at the QD GS and QD ES, respectively. Here, the energy ranges of 0.98–1.02 eV and 1.06–1.11 eV are defined as the QD GS and QD ES, respectively. To investigate the effect of the GaNAs spin filter on the performance of the electric-field-effect optical spin device using InAs QDs, the corresponding results for the InGaAs QW-InAs QD tunnel-coupled structures are also shown for reference. The PL results of the InGaAs QW-InAs QD tunnel-coupled structures with bias voltages of −2 V and 0.2 V can be found in Fig. S4. Although the variation of the PL polarization by bias voltage is extremely small for the reference sample, from 0% to 2% at the QD GS and from 1% to 4% at the QD ES, the PL polarization significantly varies with the bias voltage at the QD GS and QD ES for the GaNAs QW-InAs QD tunnel-coupled

structure. This result clearly demonstrates that the GaNAs QW spin filter is a key material for the enhanced modulation of electron spin polarization in InAs QDs at RT.

There is a significant difference in the PL polarization change between the QD GS and QD ES [Figs. 2(c) and 2(d)]. While the PL polarization increased from 7% at −2 V to 19% at 0 V for the QD GS, it increased even more significantly (from 15% to 40%) for the QD ES. This energy-dependent PL polarization at 0 V can be interpreted by considering the contribution of the GaNAs spin filter to the QD PL. Around at 0 V, the electron wavefunction can be strongly coupled between GaNAs and the QD ES [Fig. 1(b)]. Therefore, we can expect that the stronger coupling of electron wavefunctions at the QD ES relative to the QD GS may be responsible for the higher PL polarization at 0 V. In fact, the increase in the PL polarization with increasing excitation power, which is characteristic of GaNAs, can be clearly observed at the QD ES, whereas no such increase in the PL polarization appears at the QD GS (Fig. S5).

On the other hand, no significant difference in the PL polarization between the QD GS and QD ES is observed at −2 V [Fig. 2(a)]. Under these conditions, the electron injection from the GaNAs QW into the QDs can be accelerated owing to the tilted potential. The accelerated electron injection into the QDs may decrease the capture probability of conduction-band electrons by deep-level defects in GaNAs, resulting in the suppression of spin filtering. In other words, both parallel and antiparallel spin electrons are likely to be injected into the QDs without being trapped by the spin-filtering defects of GaNAs. These results indicate that the spin-filtering efficiency of a GaNAs QW can be controlled by changing the bias voltage.

To investigate the mechanism of the bias-voltage-dependent PL polarization at the QD ES in more detail, time-resolved analysis of the QD PL was performed while applying a bias voltage. Figs. 3(a) and 3(b) show the circularly-polarized PL time profiles and the corresponding PL polarizations of the QD ES at bias voltages of −2 V and 0.2 V, respectively. At −2 V, the PL polarization initially increased from ~20% to a maximum of ~30% after 50 ps, and then gradually decreased to 0 % after 150 ps due to the spin relaxation inside the QDs. In contrast, a significant increase in the PL polarization was observed under a bias voltage of 0.2 V from ~20% to ~60% after 70 ps. The magnitude of the PL polarization amplification can be attributed to the σ^+-PL decay time (τ_{σ^+}) being longer than the σ^--PL decay time (τ_{σ^-}).[31,33]

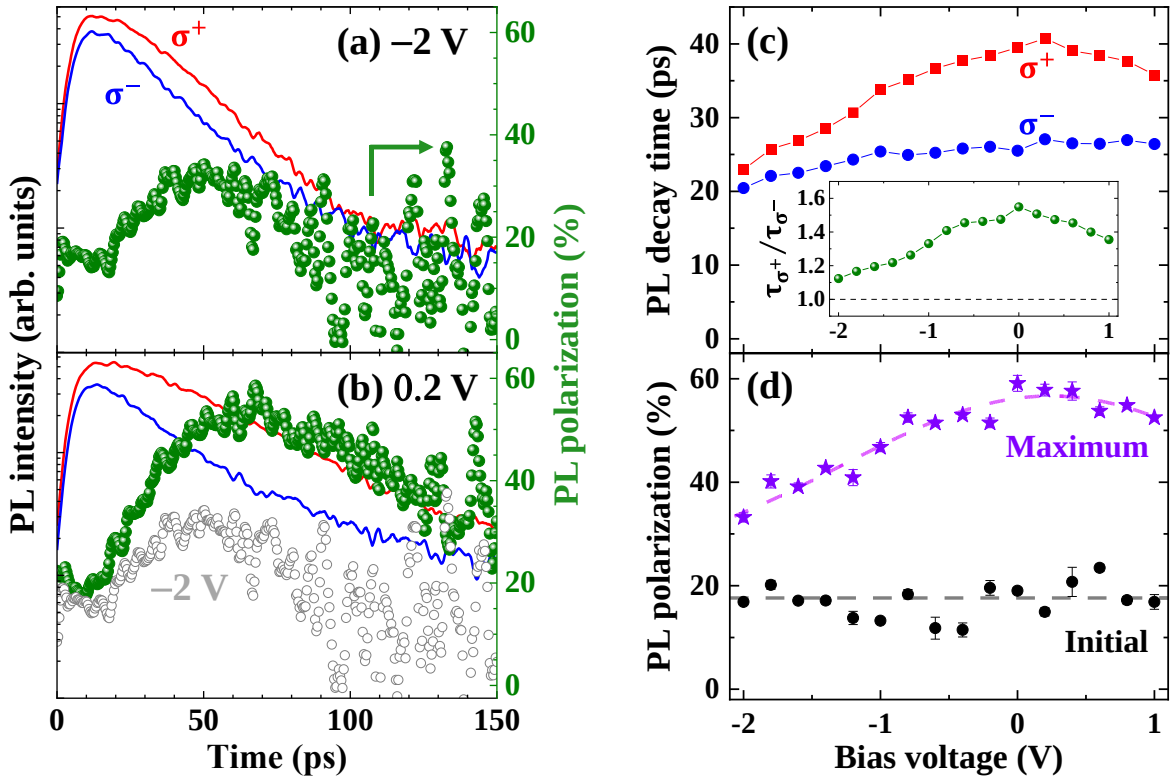


Fig. 3 Bias voltage dependence of transient QD PL polarization. Circularly-polarized PL time profiles and corresponding PL polarization of QD ES at bias voltages of (a) –2 V and (b) 0.2 V. The gray symbols shown in (b) indicate the PL polarization at a bias voltage of –2 V for comparison. (c) Bias voltage dependence of σ^+-PL decay time (τ_{σ^+}) and σ^--PL decay time (τ_{σ^-}). The inset shows how the ratio $\tau_{\sigma^+}/\tau_{\sigma^-}$ depends on the bias voltage. (d) Bias voltage dependence of maximum and initial PL polarization, deduced from the time-resolved analysis of PL polarization. The purple and gray dashed lines indicate guide lines.

This result suggests that the removal of antiparallel-spin electrons from the QDs to the GaNAs spin filter and the reinjection of parallel-spin electrons from GaNAs into QDs is efficient. The bias voltage dependences of $\tau_{\sigma^{\pm}}$ and the corresponding $\tau_{\sigma^+}/\tau_{\sigma^-}$ ratio are shown in Fig. 3(c). Here, the time range for the fitting of $\sigma^{\pm}$-PL decay was set as 20–100 ps. Although a large difference in the decay time between τ_{σ^+} (41 ps) and τ_{σ^-} (27 ps) was obtained at 0.2 V, the difference gradually decreased as the negative bias voltage increased ($\tau_{\sigma^{+(-)}}$ = 23 ps (20 ps) at −2 V). This small difference originates from a significant decrease in τ_{σ^+} relative to τ_{σ^-}, which means that the parallel-spin electrons are likely to escape from the QD ES at −2 V. When $\tau_{\sigma^+}/\tau_{\sigma^-} > 1$, spin filtering of GaNAs dominates the spin relaxation inside the QDs.[31] In this study, $\tau_{\sigma^+}/\tau_{\sigma^-} > 1$ was observed for all bias voltages ranging from −2 V to 1 V. In other words, spin filtering of GaNAs was activated regardless of the bias voltage. However, $\tau_{\sigma^+}/\tau_{\sigma^-}$ changes significantly from 1.12 at −2 V to 1.51 at 0.2 V. This result demonstrates that the spin-filtering efficiency of the GaNAs QW depends on the bias voltage.

The bias-voltage-dependent spin-filtering efficiency of GaNAs can vary the degree of spin amplification at the QD ES. Fig. 3(d) shows the maximum and initial PL polarizations as a function of the bias voltage obtained from the time-resolved analysis of the PL polarization. The maximum PL polarization increased gradually from 33% at −2 V to 59% at 0 V and then decreased slightly to 52% at 1 V. This trend is similar to the bias voltage dependence of the decay time ratio $\tau_{\sigma^+}/\tau_{\sigma^-}$. The slight decrease in the maximum PL polarization above 0 V can be attributed to the increased transfer of parallel-spin electrons from the QDs to GaNAs, as reflected by the slight decrease in τ_{σ^+} [see Fig. 3(c)]. Notably, the initial PL polarization was almost independent of the bias voltage. This result indicates that the initial PL polarization had no contribution from the GaNAs QW spin filter. A previous time-resolved PL study of GaNAs QW-InGaAs QD tunnel-coupled structures demonstrated that the PL intensity rises much faster than the increase in the PL polarization, which reflects the direct spin injection from the GaAs barrier into the QDs.[35] Therefore, we can conclude that the initial PL polarization of

approximately 15–20% is mainly affected by the direct spin injection from the GaAs barrier. This initial PL polarization, which is much lower than the initial spin polarization of 50% generated in the GaAs barrier, can be attributed to DP spin relaxation in GaAs before injection into the QDs.[7,8] This means that the time-dependent PL behaviors include electron spin injection from both the GaAs barrier and the GaNAs QW. Each component must be separated to clarify the contribution of the GaNAs QW to the QD PL polarization properties.

To separate the electron spin injection from the GaAs barrier and from the GaNAs QW, we performed rate-equation analysis considering two spin injection processes – a direct injection from the GaAs barrier into the QD ES, and a tunnel injection from the GaNAs QW into the QD ES (including a capture from the GaAs barrier) – as schematically illustrated in Fig. 4(a). The initial number of excitons generated in the GaAs barrier (GaNAs QW) with σ^+-polarization can be expressed by $N_{1(2)}$. The rate equation can be written as follows:

$$\frac{dN_{br}}{dt} = -\alpha_1 \frac{N_{br}}{\tau_{inj1}} - (1-\alpha_1)\frac{N_{br}}{\tau_{inj1}}, \quad (1)$$

$$\frac{dN_{qw}}{dt} = -\alpha_2 \frac{N_{qw}}{\tau_{inj2}} - (1-\alpha_2)\frac{N_{qw}}{\tau_{inj2}}, \quad (2)$$

$$\frac{dN_{qd1}^{\sigma+}}{dt} = \alpha_1 \frac{N_{br}}{\tau_{inj1}} - \frac{N_{qd1}^{\sigma+}}{\tau_s} - \frac{N_{qd1}^{\sigma+}}{\tau_{r1}} + \frac{N_{qd1}^{\sigma-}}{\tau_s}, \quad (3)$$

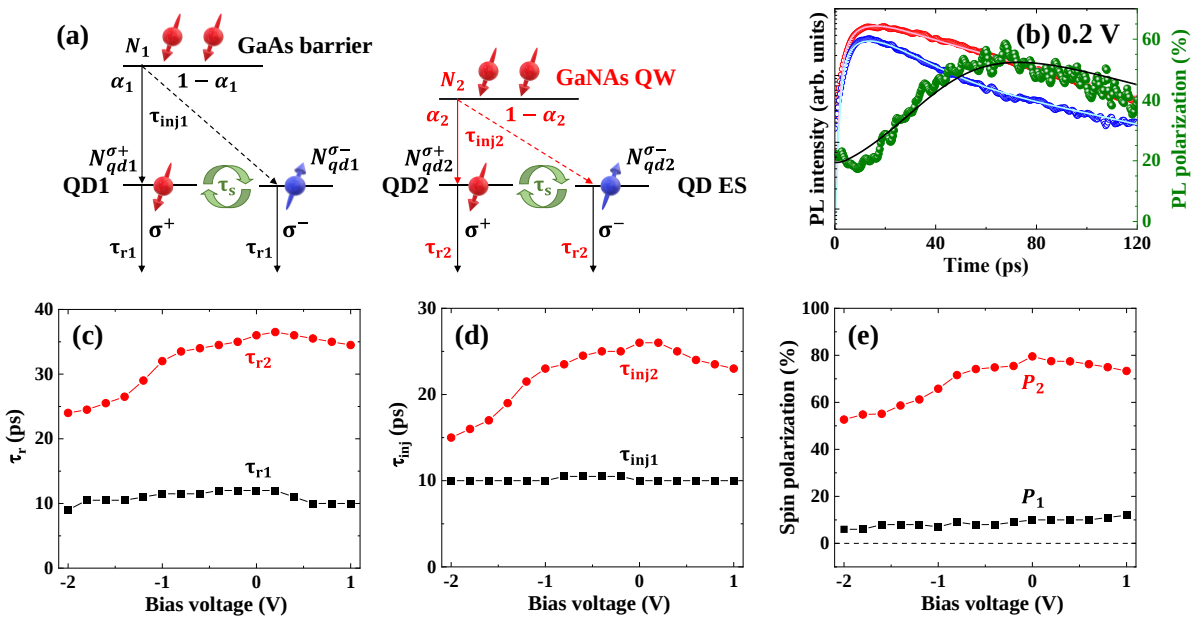


Fig. 4 Rate-equation fitting analysis considering two spin injection processes. (a) Schematic model of spin-split rate equation, where the spin injection into the QD ES from the GaAs barrier and the GaNAs QW is considered. (b) Fitted results of the rate equation for transient PL and PL polarization curves at a bias voltage of 0.2 V. Bias-voltage-dependence of time constants for (c) energy relaxation from the QD ES, $\tau_{r1,2}$, (d) spin injection into the QD ES, $\tau_{inj1,2}$, and (e) initial spin polarization of injected electrons $P_{1,2}$, defined by $100(2\alpha_{1,2}-1)$, where $\alpha_{1,2}$ is a spin conservation factor during the electron injection into the QD ES, deduced from the rate-equation fitting.

$$\frac{\mathrm{d}N_{qd2}^{\sigma^+}}{\mathrm{dt}} = \alpha_2 \frac{N_{\mathrm{qw}}}{\tau_{\mathrm{inj2}}} - \frac{N_{qd2}^{\sigma^+}}{\tau_{\mathrm{s}}} - \frac{N_{qd2}^{\sigma^+}}{\tau_{\mathrm{r2}}} + \frac{N_{qd2}^{\sigma^-}}{\tau_{\mathrm{s}}}, \quad (4)$$

$$\frac{\mathrm{d}N_{qd1}^{\sigma^-}}{\mathrm{dt}} = (1-\alpha_1) \frac{N_{\mathrm{br}}}{\tau_{\mathrm{inj1}}} - \frac{N_{qd1}^{\sigma^-}}{\tau_{\mathrm{s}}} - \frac{N_{qd1}^{\sigma^-}}{\tau_{\mathrm{r1}}} + \frac{N_{qd1}^{\sigma^+}}{\tau_{\mathrm{s}}}, \quad (5)$$

$$\frac{\mathrm{d}N_{qd2}^{\sigma^-}}{\mathrm{dt}} = (1-\alpha_2) \frac{N_{\mathrm{qw}}}{\tau_{\mathrm{inj2}}} - \frac{N_{qd2}^{\sigma^-}}{\tau_{\mathrm{s}}} - \frac{N_{qd2}^{\sigma^-}}{\tau_{\mathrm{r2}}} + \frac{N_{qd2}^{\sigma^+}}{\tau_{\mathrm{s}}}, \quad (6)$$

where the excitons generated in the GaAs barriers (GaNAs QW) are injected into the QD ES with a time constant of $\tau_{\mathrm{inj1(inj2)}}$. Since the evaluation of the spin polarization degree of electrons injected from the GaNAs QW is important in this study, the spin conservation factor during injection is introduced. The parameter of $\alpha_{1(2)}$ is defined as the spin conservation factor during the injection of electrons from the GaAs barrier (GaNAs QW) into the QD ES. In other words, α_1 and α_2 depend on the degree of spin relaxation in the GaAs barrier and spin filtering in the GaNAs QW, respectively. It is assumed that the spin polarization of electrons is conserved during tunneling between the GaNAs QW and QD. Here, note that $\alpha_{1,2}$ indicates the fraction of spin conservation, where a value of 0.5 (0.75) indicates that the spin polarization of injected electrons $P_{1,2}$ is 0% (50%). In this model, the parallel-spin electrons $\alpha_1 N_1$ ($\alpha_2 N_2$) are injected from the GaAs barrier (GaNAs QW) into the parallel-spin state of the QD ES, whereas the antiparallel-spin electrons $(1-\alpha_1)N_1$ $[(1-\alpha_2)N_2]$ are injected into the opposite spin state. The spin-polarized electrons injected into the QD ES relax with a time constant of the conventional spin relaxation (τ_{s}) and with a time constant of $\tau_{\mathrm{r1,2}}$. The parameter of $\tau_{\mathrm{r1,2}}$ can be expressed by the radiative and nonradiative decay processes, as follows:

$$\frac{1}{\tau_{\mathrm{r1(r2)}}} = \frac{1}{\tau_{\mathrm{rad}}} + \frac{1}{\tau_{\mathrm{nr1(nr2)}}}, \quad (7)$$

where $\tau_{\mathrm{nr1,2}}$ mainly includes the trapping in the deep-level defects of GaNAs QW via tunnel transfer from the QD ES to the GaNAs QW except the thermal excitation (escape) and energy relaxation into the lower-energy states. Here, note that $\tau_{\mathrm{r1,2}}$ can also reflect the reinjection

process of electrons from the GaNAs QW into the QD ES, as discussed below. Fig. 4(b) shows the fitted results of this rate equation for the transient PL and PL polarization curves at 0.2 V, combined with a convolution calculation of the time-response curve for the excitation laser pulse. The slow amplification of the PL polarization and the characteristic PL decay features were well expressed by the fitted results. Optimization of the three main fitting parameters, τ_{r2}, τ_{inj2}, and α_2 illustrated all of the PL time profiles and the resulting PL polarization behavior.

Fig. 4(c) shows the bias voltage dependence of $\tau_{r1,2}$, deduced from the fitting of the above rate-equation. Across all bias voltage ranges, τ_{r1} was much shorter than τ_{r2}. As described above, spin-polarized deep-level defects in GaNAs can selectively capture antiparallel-spin electrons due to Pauli blocking. Because the spin polarization of electrons directly injected from the GaAs barrier into the QDs is significantly low, owing to DP spin relaxation in GaAs,[7,8] the capture of electron spins by deep-level defects via a tunnel transfer from the QD ES to the GaNAs QW is likely to occur. This dominant electron transfer from the QD ES to the GaNAs QW can lead to τ_{r1} which is shorter than τ_{r2}. In contrast, τ_{r2} increases gradually from 24 ps at −2 V to 36 ps at 0 V. No significant change in τ_{r2} was observed from 0 to 1 V. This trend is similar to the bias voltage dependence of the σ^+-PL decay time [see Fig. 3(c)]. Here, the spin polarization of the electrons injected from the GaNAs QW into the QD ES can be amplified by spin filtering in GaNAs. This injection of highly spin-polarized electrons can promote the reinjection of parallel-spin electrons via blocked energy relaxation to the spin-polarized defects in GaNAs, resulting in a longer τ_{r2} for a bias voltage at approximately 0 V. The decrease in τ_{r2} at a large negative bias voltage of −2 V can be mainly attributed to electron tunnelling escape from the QD ES to the GaAs capping layer via thermal excitation, as discussed above.

The bias voltage dependence of $\tau_{inj1,2}$ is plotted in Fig. 4(d). As in the case for $\tau_{r1,2}$, τ_{inj1} is significantly shorter than τ_{inj2}. This is because of the direct injection from the GaAs barrier into the QDs without being captured by the GaNAs QW. It should be noted that τ_{inj2} is strongly

affected by the bias voltage. τ_{inj2} increased from 15 ps at −2 V to 26 ps at 0 V, and then slightly decreased to 23 ps at 1 V. The shorter τ_{inj2} value at −2 V, which is close to τ_{inj1} = 10 ps, suggests rapid electron injection from the GaNAs QW into the QD ES owing to the potential tilted towards the QDs. This accelerated electron injection can suppress spin filtering in GaNAs, leading to a decreased spin polarization degree of the injected electrons [Fig. 4(e)]. On the other hand, τ_{inj2} increases as the band potential approaches flat owing to the decrease in the negative bias voltage. In this case, spin filtering in the GaNAs QW was promoted, enhancing the spin polarization degree of the injected electrons. The spin polarization degree of electrons injected from the GaNAs QW into the QD ES was found to vary from 53% to 80% depending on the bias voltage, in comparison with the almost constant spin polarization degree of electrons injected from the GaAs barrier (~10%). In this study, the initial spin polarization of the electrons generated in the GaAs barrier was expected to be 50% according to the optical-transition selection rule. Therefore, this result indicates that the degree of spin amplification in GaNAs can be controlled by changing the bias voltage. These findings demonstrate that the bias-voltage-dependent QD PL polarization (in the range of 15–40%) can be mainly attributed to the change in the amplified spin polarization of electrons injected from the GaNAs QW.

Finally, the electric-field dependence of the spin-filtering dynamics in the GaNAs QW-InAs QD tunnel-coupled structure is discussed. To clarify it, three-dimensional calculations of the coupled electron wavefunctions of the QD ES at different bias voltages were performed using nextnano software.[34] The details of the calculation model are described in the Experimental Section. Figs. 5(a) and 5(b) show the existence probabilities of the coupled electron wavefunctions along the z-axis together with the conduction-band profiles at bias voltages of −2 V and 0.2 V, respectively. The spread of the QD ES electron wavefunction over the GaNAs QW is much weaker at a bias voltage of −2 V than that at 0.2 V. At negative bias voltages, the QW-QD conduction-band potential tilts toward the QD side, which can induce the localization of electrons in the QD. This weak coupling should suppress the injection (or reinjection) of spin-filtered electrons from the GaNAs QW into the QD ES. In addition, the conduction-band potential tilted toward the QD side can accelerate electron injection into the QD ES. This decreases the capture probability of electron spins by deep-level defects in GaNAs, resulting in the suppression of spin filtering [Fig. 5(a)]. In this case, the spin polarization degree of the electrons injected from the GaNAs QW into the QD ES is reduced, and thus the PL polarization becomes lower. Furthermore, even if highly spin-polarized electrons are injected

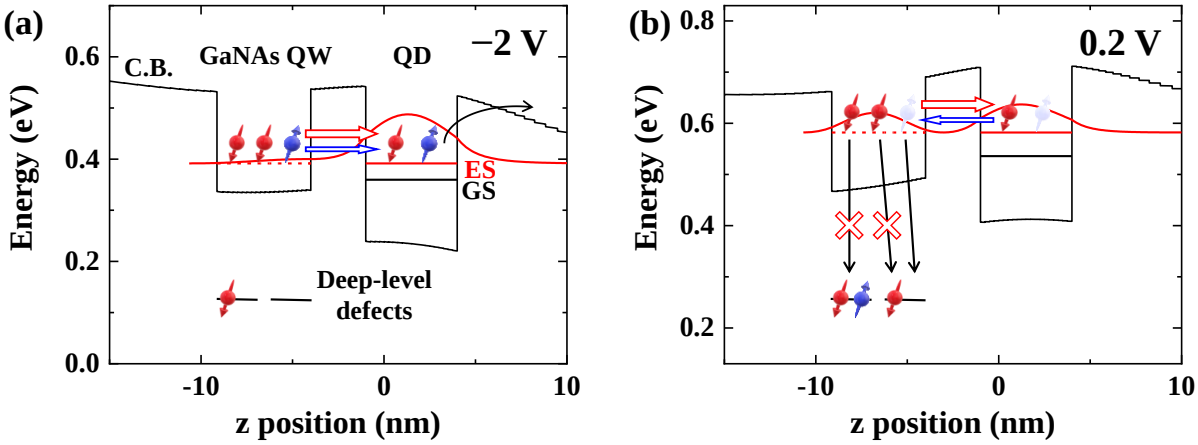


Fig. 5 Electric-field dependence of spin filtering dynamics in the GaNAs QW-InAs QD tunnel-coupled structure. Schematic illustrations of electron spin dynamics, together with the three-dimensional calculated band profiles, and the existence probabilities of the coupled electron wavefunctions of the QD ES at bias voltages of (a) −2 V, and (b) 0.2 V. The energy positions of deep-level defects in GaNAs are hypothetical.

307 into the QD ES, they can easily tunnel and escape to the GaAs capping layer via thermal
308 excitation. As a result, the dominant escape of parallel-spin electrons from the QD ES could
309 effectively cancel the contribution of the GaNAs spin filter for QD PL polarization.

310 On the other hand, at a bias voltage of 0.2 V, the electron wavefunction of the QD ES
311 significantly spreads over the GaNAs QW [see Fig. 5(b)]. This strong coupling promotes not
312 only the injection (reinjection) of parallel-spin electrons from the GaNAs QW to the QD ES,
313 but also the selective transfer of antiparallel-spin electrons from the QD ES to the GaNAs QW.
314 A nearly flat band potential is reached in this bias condition, and thus the spin injection into the
315 QD ES becomes slower, as compared to that at −2 V. This increases the capture probability of
316 electron spins by defects in GaNAs [see Fig. 5(b)]. In this case, even a slight spin polarization
317 of the electrons injected from the GaAs barrier into the GaNAs QW can cause an SDR process,
318 resulting in a dynamic spin polarization of the electrons localized at the spin-filtering defects.[36]
319 The SDR process drives both conduction-band electrons and defect electrons towards the
320 parallel-spin orientation. The resulting spin-polarized defects can selectively capture
321 antiparallel-spin electrons due to Pauli blocking, thereby enhancing the spin polarization of
322 conduction-band electrons. As a result, highly spin-polarized electrons are efficiently injected
323 into the QD ES, resulting in higher PL polarization. Spin filtering in GaNAs is known to be
324 thermally activated because of the thermally-accelerated capture of electron spins by deep-level
325 defects.[31] Because the energy difference between the defect level and conduction-band edge is
326 sufficiently larger than the thermal energy at RT, spin filtering is expected to be stable even
327 above RT. This means that the studied GaNAs QW-InAs QD tunnel-coupled structure is a
328 promising opto-semiconductor nanostructure for practical electric-field-effect optical spin
329 devices. Finally, we discuss the applicability of such a spin-filtering system to two-dimensional
330 materials, which are the promising candidates for future opto-electronic and spintronic
331 devices.[37] For transition metal dichalcogenides (TMDCs) such as MoS_2[38] and WS_2,[39] spin
332 polarization of the optically excited carries higher than 60% has been observed at RT via

circularly polarized PL spectroscopy. It has recently been reported in these materials that deep-level defects can be introduced in the band gap.[40,41] If these defects behave as spin-filtering defects as in GaNAs and their spin-filtering efficiency can be controlled using an electric field, it would be possible to vary the spin polarization even more widely. In addition, integration of photochromic materials into such an electric-field-effect optical spin device may provide a novel functionality for opto-electronic device applications.[42]

Conclusions

In summary, we demonstrated the enhanced RT electric field control of PL polarization at the QD ES in the range of 15–40% using the GaNAs QW-InAs QD tunnel-coupled structure, in comparison with the PL polarization in the range of 1–4% for the InGaAs QW-InAs QD tunnel-coupled structure. This achievement is attributed to the electric-field-dependent spin polarization of the electrons injected from the GaNAs QW into the QD ES. By changing the coupled-band potential with the bias voltage, the spin-injection time from the GaNAs QW into the QD ES can be varied, thereby controlling the capture probability of electrons by spin-polarized deep-level defects in GaNAs, that is, the spin-filtering efficiency. These results provide a new method for electric-field modulation of optical spin polarization by switching spin amplification. Electric field control of the spin-filtering dynamics in GaNAs and the resultant optical spin polarization in InAs QDs will facilitate the practical applications of semiconductor opto-spintronics, in which the electric field control of electron spin information is an essential prerequisite.

Materials and methods

Molecular beam epitaxy growth and device fabrication

The electric-field-effect optical spin device schematically depicted in Fig. 1(a) was grown using an EIKO molecular beam epitaxy system on a p-doped GaAs(100) substrate (supplied by Wafer Technology Ltd. (UK)). The active layer was composed of a single layer of InAs QDs, tunnel-coupled with a 5-nm-thick GaNAs QW. The GaNAs QW was grown on a 100-nm-thick GaAs layer at 400 °C using a radio frequency (RF) plasma source for nitrogen (Oxford Applied Research Model MPD21). Self-assembled 3.8-ML-thick InAs QDs were grown at 480 °C after the growth of a 3-nm-thick GaAs tunneling barrier at 580 °C, and capped with 10-nm-thick undoped GaAs at 480 °C. The other GaAs and $Al_{0.2}Ga_{0.8}As$ barrier layers were grown at 580 °C. The nitrogen content of the GaNAs QW was set to 0.9% by adjusting the growth conditions of the RF power and N_2 flow rate. An Fe/Au electrode was deposited on top, and a 10 μm square optical window was fabricated using standard photolithography and etching techniques for optical spin excitation and PL observations. Reference InAs QD samples were prepared under identical growth conditions in this study, and additional QDs were grown on top for structural characterization via atomic force microscopy (AFM).

Structural characterization of QDs

Scanning transmission electron microscopy (STEM) samples were prepared via a standard bulk-pick-up method using a focused ion beam instrument (JIB-4600F, JEOL). STEM observations were performed using an aberration-corrected FEI-Titan cubic electron microscope (Titan3 G2 60-300, FEI Co.). High-angle annular dark-field (HAADF) STEM imaging was used to observe buried QDs in the reference samples. A typical HAADF-STEM image exhibits a QD structure with a diameter and height of 25 and 4 nm, respectively (Fig. S6). The QD diameter obtained was the same as that obtained by AFM, as described below.

The areal density and size distribution of the QDs were evaluated using atomic force microscopy (AFM, SPI-3800, Seiko Instruments Inc.). AFM analysis revealed an areal density

of 2.3×10^{10} cm^{-2} with an average diameter of 25 nm (Fig. S3). Because the lateral resolution of AFM is limited by tip sharpness,[43] a curvature radius of 3 nm for the ultra-sharp tip (SI-DF20S, SII NanoTechnology) was considered for the analysis.

Polarization- and time-resolved optical characterization

Circularly polarized PL was detected using a cooled InGaAs detector (iDus DU490A, Andor) through a spectrometer (Kymera-328i, Andor) under σ^+-polarized excitation at 295 K. Both the excitation and detection directions coincided with the sample growth direction. A quarter-wave plate with a linear polarizer was used to create (detect) circularly polarized excitation (emission). A wavelength-tunable pulsed laser with a repetition rate of 80 MHz and pulse width of less than 120 fs (InSight X3, Spectra-Physics) was used as the excitation source. The excitation laser was focused to a spot size ~20 μm in diameter using a microscope objective lens. The excitation wavelength was set to 850 nm (~1.46 eV) for excitation of the GaAs barrier, where the initial spin polarization degree of the generated electrons was expected to be 50% according to the optical-transition selection rule.[6] The excitation laser power density was set at approximately 30 μW μm^{-2}. The circularly-polarized PL emitted from the QDs reflects the spin polarization of electrons in the QD emissive states,[27] and the PL polarization is defined as follows:

$$P_{PL} = (I_{\sigma^+} - I_{\sigma^-})/(I_{\sigma^+} + I_{\sigma^-}), \quad (8)$$

where $I_{\sigma^\pm}$ denotes the co- and cross-circularly polarized PL intensities with σ^+-polarized excitation. In this work, spin-polarized carriers are predominantly generated in a 100-nm-thick GaAs layer grown below the 5-nm-thick GaNAs QW, considering the penetration depth of the excitation laser of ~800 nm. The generated spin-polarized carriers are directly injected into the QDs or injected from the GaNAs QW into the QDs via thermally-stable spin-conserved tunneling after carrier capture by the GaNAs QW.[44,45]

Circularly-polarized time-resolved PL was measured using a streak camera (C10910-02, Hamamatsu Photonics) combined with a spectrometer (C11119-04, Hamamatsu Photonics)

under a pulsed σ^+-polarized excitation at 295 K. A mode-locked Ti:Sapphire pulsed laser with a repetition rate of 80 MHz and a pulse width of less than 100 fs (Mai Tai HP, Spectra-Physics) was used as the excitation source, and the excitation wavelength was set to 850 nm (~1.46 eV). The excitation laser power density was set at approximately 50 μW μm^{-2}. The full width at half maximum of the laser pulse time-response curve was 4 ps.

Band potential calculation

Three-dimensional calculations of the band potential and wavefunctions for the GaNAs QW-InAs QD tunnel-coupled structure under an electric field were performed using nextnano software.[34] Here, one-dimensional calculations of the band potential for the entire device structure were performed before three-dimensional calculations to determine the electric field applied around the QW-QD tunnel-coupled structure at each bias voltage. In general, the In composition of QDs is known to decrease due to In-Ga intermixing during the capping process of the QDs,[46] and thus, InGaAs QDs are inevitably formed. In this calculation, the In composition of the InGaAs QDs was set to 0.65 to match the RT PL peak at around 1.02 eV (QD GS) shown in Figs. 2(a) and 2(b). In addition, the calculation model assumes a 1-nm-thick wetting layer, one truncated pyramidal QD with a base length of 25 nm, and a height of 4 nm, considering the uniform In composition inside the QD and the influence of strain on the local band structure. The structural model is based on AFM and STEM observations of the reference QDs described above. The nitrogen content of the 5-nm-thick GaNAs QW was set to 0.9%.

Author contributions

Soyoung Park: Conceptualization, Data curation, Formal analysis, Investigation, Methodology, Visualization, Writing – original draft. Satoshi Hiura: Conceptualization, Data curation, Formal analysis, Funding acquisition, Investigation, Methodology, Project administration, Supervision, Writing – review & editing. Hiroto Kise: Formal analysis, Investigation, Writing – review & editing. Junichi Takayama: Formal analysis, Investigation, Software, Writing – review &

editing. Kazuhisa Sueoka: Writing – review & editing. Akihiro Murayama: Conceptualization, Funding acquisition, Methodology, Project administration, Supervision, Writing – review & editing.

Conflicts of interest

There are no conflicts to declare.

Acknowledgements

This work was supported by JSPS KAKENHI (Grant No. JP16H06359, No. JP19K15380, No. JP20K20433, No. JP21H01356, and No. JP21KK0068), JST FOREST (Grant No. JPMJFR202E), and the Advanced Technology Institute Research Grant 2021, Murata Science Foundation. Part of this work was conducted at Hokkaido University, supported by the "Nanotechnology Platform Program" of the Ministry of Education, Culture, Sports, Science, and Technology (MEXT), Japan (Grant No. JPMXP09F20HK0010).

References

1. S. A. Wolf, D. D. Awschalom, R. A. Buhrman, J. M. Daughton, S. von Molnár, M. L. Roukes, A. Y. Chtchelkanova and D. M. Treger, Spintronics: A Spin-Based Electronics Vision for the Future, *Science* 2001, **294**, 1488–1495.
2. I. Žutić, J. Fabian and S. Das Sarma, Spintronics: Fundamentals and Applications, *Rev. Mod. Phys.* 2004, **76**, 323–410.
3. D. D. Awschalom and M. E. Flatté, Challenges for Semiconductor Spintronics, *Nat. Phys.* 2007, **3**, 153–159.
4. J. Tang and K. L. Wang, Electrical Spin Injection and Transport in Semiconductor Nanowires: Challenges, Progress and Perspectives, *Nanoscale* 2015, **7**, 4325–4337.

5. W. Kang, Y. Zhang, Z. Wang, J.-O. Klein, C. Chappert, D. Ravelosona, G. Wang, Y. Zhang and W. Zhao, Spintronics, *ACM J. Emerg. Technol. Comput. Syst.* 2015, **12**, 1–42.

6. *Optical Orientation*, ed. F. Meier and B. P. Zakharchenya, North Holland, Amsterdam, 1984.

7. M. I. D'yakonov and V. I. Perel', Spin Orientation of Electrons Associated With the Interband Absorption of Light in Semiconductors, *Zh. Eksp. Teor. Fiz* 1971, **60**, 1954–1965.

8. M. I. D'yakonov and V. Yu. Kachorovskii, Spin Relaxation of Two-Dimensional Electrons in Noncentrosymetric Semiconductors, *Fiz. Tekh. Poluprovodn.* 1986, **20**, 178–181.

9. R. J. Elliott, Theory of the Effect of Spin-Orbit Coupling on Magnetic Resonance in Some Semiconductors, *Phys. Rev.* 1954, **96**, 266–279.

10. Y. Yafet, g Factors and Spin-Lattice Relaxation of Conduction Electrons, *Solid State Phys.* 1963, **14**, 1–98.

11. G. L. Sir, A. G. Aronov and G. E. Pikus, Spin Relaxation of Electrons Due to Scattering by Holes, *Zh. Eksp. Teor. Fiz* 1975, **69**, 13821397.

12. A. V. Khaetskii and Y. V. Nazarov, Spin Relaxation in Semiconductor Quantum Dots, *Phys. Rev. B* 2000, **61**, 12639–12642.

13. J. M. Elzerman, R. Hanson, L. H. Willems van Beveren, B. Witkamp, L. M. K. Vandersypen and L. P. Kouwenhoven, Single-Shot Read-out of an Individual Electron Spin in a Quantum Dot, *Nature* 2004, **430**, 431–435.

14. M. Kroutvar, Y. Ducommun, D. Heiss, M. Bichler, D. Schuh, G. Abstreiter and J. J. Finley, Optically Programmable Electron Spin Memory Using Semiconductor Quantum Dots, *Nature* 2004, **432**, 81–84.

15. M. J. Martín-Sánchez, G. Muñoz-Matutano, J. Herranz, J. Canet-Ferrer, B. Alén, Y. González, P. Alonso-González, D. Fuster, L. González, J. Martínez-Pastor and F. Briones,

Single Photon Emission from Site-Controlled InAs Quantum Dots Grown on GaAs(001) Patterned Substrates, *ACS Nano* 2009, **3**, 1513–1517.

16. Y. Yang, Y. Zheng, W. Cao, A. Titov, J. Hyvonen, J. R. Manders, J. Xue, P. H. Holloway and L. Qian, High-Efficiency Light-Emitting Devices Based on Quantum Dots with Tailored Nanostructures, *Nat. Photonics* 2015, **9**, 259–266.

17. A. Jaffal, W. Redjem, P. Regreny, H. S. Nguyen, S. Cueff, X. Letartre, G. Patriarche, E. Rousseau, G. Cassabois, M. Gendry and N. Chauvin, InAs Quantum Dot in a Needlelike Tapered InP Nanowire: a Telecom Band Single Photon Source Monolithically Grown on Silicon, *Nanoscale* 2019, **11**, 21847–21855.

18. R. Beaulac, P. I. Archer, S. T. Ochsenbein and D. R. Gamelin, Mn^{2+}-Doped CdSe Quantum Dots: New Inorganic Materials for Spin-Electronics and Spin-Photonics, *Adv. Funct. Mater.* 2008, **18**, 3873–3891.

19. R. Beaulac, L. Schneider, P. I. Archer, G. Bacher and D. R. Gamelin, Light-Induced Spontaneous Magnetization in Doped Colloidal Quantum Dots, *Science* 2009, **325**, 973–976.

20. L. Turyanska, J. H. Blokland, U. Elfurawi, O. Makarovsky, P. C. M. Christianen and A. Patanè, Photoluminescence of PbS Nanocrystals at High Magnetic Fields up to 30 T, *Phys. Rev. B* 2010, **82**, 193302.

21. J. H. Yu, X. Liu, K. E. Kweon, J. Joo, J. Park, K.-T. Ko, D. W. Lee, S. Shen, K. Tivakornsasithorn, J. S. Son, J.-H. Park, Y.-W. Kim, G. S. Hwang, M. Dobrowolska, J. K. Furdyna and T. Hyeon, Giant Zeeman Splitting in Nucleation-Controlled Doped CdSe:Mn^{2+} Quantum Nanoribbons, *Nat. Mater.* 2010, **9**, 47–53.

22. K. Zhang, J. Zhao, Q. Hu, S. Yang, X. Zhu, Y. Zhang, R. Huang, Y. Ma, Z. Wang, Z. Ouyang, J. Han, Y. Han, J. Tang, W. Tong, L. Zhang and T. Zhai, Room-Temperature Magnetic Field Effect on Excitonic Photoluminescence in Perovskite Nanocrystals, *Adv. Mater.* 2021, **33**, 2008225.

510 23. S. Cortez, O. Krebs, S. Laurent, M. Senes, X. Marie, P. Voisin, R. Ferreira, G. Bastard,
511 J.-M. Gérard and T. Amand, Optically Driven Spin Memory in n-Doped InAs-GaAs
512 Quantum Dots, *Phys. Rev. Lett.* 2002, **89**, 207401.
513 24. A. Shabaev, E. A. Stinaff, A. S. Bracker, D. Gammon, A. L. Efros, V. L. Korenev and I.
514 Merkulov, Optical Pumping and Negative Luminescence Polarization in Charged GaAs
515 Quantum Dots, *Phys. Rev. B* 2009, **79**, 035322.
516 25. H. Chen, S. Hiura, J. Takayama, S. Park, K. Sueoka and A. Murayama, Electric Field
517 Control of Spin Polarity in Spin Injection into InGaAs Quantum Dots from a Tunnel-
518 Coupled Quantum Well, *Appl. Phys. Lett.* 2019, **114**, 133101.
519 26. S. Park, H. Chen, S. Hiura, J. Takayama, K. Sueoka and A. Murayama, Electric-Field-
520 Effect Spin Switching with an Enhanced Number of Highly Polarized Electron and
521 Photon Spins Using p-Doped Semiconductor Quantum Dots, *ACS Omega* 2021, **6**, 8561–
522 8569.
523 27. S. Park, S. Hiura, J. Takayama, K. Sueoka and A. Murayama, Efficient Room-
524 Temperature Voltage Control of Picosecond Optical Spin Orientation Using a III-V
525 Semiconductor Nanostructure, *Adv. Electron. Mater*. 2022, **8**, 2200588.
526 28. S. Hiura, M. Takishita, J. Takayama, S. Sato and A. Murayama, Highly Efficient Room-
527 Temperature Electron-Photon Spin Conversion Using a Semiconductor Hybrid
528 Nanosystem with Gradual Quantum Dimensionality Reduction, *Phys. Rev. Appl.* 2020,
529 **14**, 044011.
530 29. S. Sato, S. Hiura, J. Takayama and A. Murayama, Temperature Dependence of Inter-Dot
531 Electron-Spin Transfer among Laterally Coupled Excited States in High-Density InGaAs
532 Quantum Dots, *J. Appl. Phys.* 2020, **127**, 043904.
533 30. S. Sato, S. Hiura, J. Takayama and A. Murayama, Suppression of Thermally Excited
534 Electron-Spin Relaxation in InGaAs Quantum Dots Using p-Doped Capping Layers

toward Enhanced Room-Temperature Spin Polarization, *Appl. Phys. Lett.* 2020, **116**, 182401.

31. Y. Huang, V. Polojärvi, S. Hiura, P. Höjer, A. Aho, R. Isoaho, T. Hakkarainen, M. Guina, S. Sato, J. Takayama, A. Murayama, I. A. Buyanova and W. M. Chen, Room-Temperature Electron Spin Polarization Exceeding 90% in an Opto-Spintronic Semiconductor Nanostructure via Remote Spin Filtering, *Nat. Photonics* 2021, **15**, 475–482.

32. V. K. Kalevich, E. L. Ivchenko, M. M. Afanasiev, A. Y. Shiryaev, A. Y. Egorov, V. M. Ustinov, B. Pal and Y. Masumoto, Spin-Dependent Recombination in GaAsN Solid Solutions, *J. Exp. Theor. Phys. Lett.* 2005, **82**, 455–458.

33. X. J. Wang, I. A. Buyanova, F. Zhao, D. Lagarde, A. Balocchi, X. Marie, C. W. Tu, J. C. Harmand and W. M. Chen, Room-Temperature Defect-Engineered Spin Filter Based on a Non-Magnetic Semiconductor, *Nat. Mater.* 2009, **8**, 198–202.

34. S. Birner, T. Zibold, T. Andlauer, T. Kubis, M. Sabathil, A. Trellakis and P. Vogl, Nextnano: General Purpose 3-D Simulations, *IEEE Trans. Electron Devices* 2007, **54**, 2137–2142.

35. K. Etou, S. Hiura, S. Park, J. Takayama, A. Subagyo, K. Sueoka and A. Murayama, Efficient Room-Temperature Operation of a Quantum Dot Spin-Polarized Light-Emitting Diode under High-Bias Conditions, *Phys. Rev. Appl.* 2023, **19**, 024055.

36. Y. Puttisong, I. A. Buyanova and W. M. Chen, Limiting Factor of Defect-Engineered Spin-Filtering Effect at Room Temperature, *Phys. Rev. B* 2014, **89**, 195412.

37. J. Zou, Y. Yang, D. Hu, L. Kang, C. Zhu, D. Tian, X. Lv, G. Kutty, Y. Guo, M. Xu, F. Li, G. Hong and Z. Liu, Controlled Growth of Ultrathin Ferromagnetic β-MnSe Semiconductor, *SmartMat*, 2022, **3**, 482–490.

38. R. Dhall, K. Seyler, Z. Li, D. Wickramaratne, M. R. Neupane, I. Chatzakis, E. Kosmowska, R. K. Lake, X. Xu and S. B. Cronin, Strong Circularly Polarized

Photoluminescence from Multilayer MoS_2 Through Plasma Driven Direct-Gap Transition, *ACS Photonics* 2016, **3**, 310–314.

39. B. Zhu, H. Zeng, J. Dai, Z. Gong and X. Cui, Anomalously Robust Valley Polarization and Valley Coherence in Bilayer WS_2, *Proc. Natl. Acad. Sci.*, 2014, **111**, 11606–11611.

40. Y. Zhao, M. Tripathi, K. Čerņevičs, A. Avsar, H. G. Ji, J. F. Gonzalez Marin, C. Y. Cheon, Z. Wang, O. V. Yazyev and A. Kis, Electrical Spectroscopy of Defect States and Their Hybridization in Monolayer MoS_2, *Nat. Commun.*, 2023, **14**, 1–9.

41. X. Xu, L. Li, M. Yang, Q. Guo, Y. Wang, X. Li, X. Zhuang and B. Liang, Localized State Effect and Exciton Dynamics for Monolayer WS_2, *Opt. Express*, 2021, **29**, 5856.

42. Y. Geng, Y. Zhao, J. Zhao, Y. Zhai, M. Yuan, X. Wang, H. Gao, J. Feng, Y. Wu and L. Jiang, Optical and Electrical Modulation in Ultraviolet Photodetectors Based on Organic One-Dimensional Photochromic Arrays, *SmartMat*, 2021, **2**, 388–397.

43. D. González, D. F. Reyes, A. D. Utrilla, T. Ben, V. Braza, A. Guzman, A. Hierro and J. M. Ulloa, General Route for the Decomposition of InAs Quantum Dots during the Capping Process, *Nanotechnology* 2016, **27**, 125703.

44. X.-J. Yang, T. Kiba, T. Yamamura, J. Takayama, A. Subagyo, K. Sueoka and A. Murayama, Ultrafast Spin Tunneling and Injection in Coupled Nanostructures of InGaAs Quantum Dots and Quantum Well, *Appl. Phys. Lett.* 2014, **104**, 012406.

45. S. L. Chen, T. Kiba, X. J. Yang, J. Takayama and A. Murayama, Temperature-Dependent Spin Injection Dynamics in InGaAs/GaAs Quantum Well-Dot Tunnel-Coupled Nanostructures, *J. Appl. Phys.* 2016, **119**, 115701.

46. T. Kaizu, T. Matsumura and T. Kita, Broadband Control of Emission Wavelength of InAs/GaAs Quantum Dots by GaAs Capping Temperature, *J. Appl. Phys.* 2015, **118**, 154301.